TWENTY-FIFTH EUROPEAN ROTORCRAFT FORUM

Paper No. C14

# Numerical Simulation of the BK117 / EC145 Fuselage Flow Field

by

Eberhard Schöll

EUROCOPTER DEUTSCHLAND GmbH, München, Germany

September 14-16, 1999

Rome

Italy

ASSOCIAZIONE INDUSTRIE PER L'AEROSPAZIO, I SISTEMI E LA DIFESA
ASSOCIAZIONE ITALIANA DI AERONAUTICA ED ASTRONAUTICA

# Numerical Simulation of the BK117 / EC145 Fuselage Flow Field

Eberhard Schöll

*EUROCOPTER DEUTSCHLAND GmbH, 81663 München, Germany*

**The need for increasing their competitiveness and reducing development times forces the helicopter industry to introduce improved aerodynamic tools for analyzing the flowfields around helicopter components. CFD methods have rapidly matured over the last few years and are now powerful enough to be integrated in the industrial design process. At EUROCOPTER DEUTSCHLAND, a commercial CFD software was installed and applied during the BK117 upgrade development program. An extensive validation by calculating the flowfield around the existing BK117 fuselage and comparing the results to wind tunnel test data was performed in order to prove the accuracy and reliability of the CFD method. The fuselage aerodynamics of the upgrade helicopter EC145 were investigated by simple wind tunnel tests measuring the aerodynamic coefficients and CFD calculations. The application of the CFD method supplemented the wind tunnel tests and provided surface pressure distributions as input for stress analysis of the fuselage structure. Furthermore, a first attempt was made to use CFD simulations for estimating the aerodynamic efficiencies of horizontal stabilizer and endplates and for simulating the influence of the rotor downwash by activating the actuator disk model of the CFD software.**

## Introduction

As time-to-market for the design and development of a new helicopter or an upgrade of an existing helicopter has to be decreased to be competitive in the world market, there is a pressing need for improved aerodynamic methodologies capable of analyzing the flowfield around helicopter components such as main rotor or fuselage and empenage in various flight conditions.

The unique ability of helicopters to hover or fly at very low speed in any directions and the unsteady operation of its rotating rotor blades generate numerous specific and complex aerodynamic problems which have permanently been challenging the engineer's skills since the pioneering flights. Up to recent times, theoretical and numerical methods were unable to satisfactorily cope with these problems and the empirical approach based on flight tests and wind tunnel tests was extensively used by the industry.

Flight tests are extremely expensive and time consuming while the solutions found are often palliatives rather than optimized configurations. The wind tunnel methodology can be more efficient for conventional problems such as fuselage drag reduction but many low speed interactional conditions have been found difficult to simulate with sufficient confidence.

Paper presented at the 25th European Rotorcraft Forum, Rome, Italy, September 14-16, 1999

CFD methods developed by the research community have rapidly matured over the last few years and are now available as powerful commercial products. Solutions with engineering accuracy for surface pressure can be obtained for realistic three-dimensional configurations such as those applicable to complete commercial aircraft. Therefore, the fixed-wing industry increasingly uses those CFD methods and has already incorporated them in its design methodology thus reducing the number of wind tunnel tests with a greater number of configurations being explored numerically.

In the rotorcraft industry, CFD applications have historically lagged behind fixed-wing applications by five to ten years due to much smaller market size, less personnel with CFD experience and higher complexity of rotorcraft aerodynamics. But the need for increasing the competitiveness has forced the helicopter industry to invest in introducing CFD methods into their design processes. Recently, first industrial CFD applications were published showing the efforts to improve the aerodynamic design of helicopter components. Hassan et al. [1] conducted Euler simulations for the isolated AH-64D™ Longbow Apache™ fuselage in order to investigate and solve tail buffeting problems in low speed descent flight. Serr and Cantillon [2] simulated air intake flowfields using a Navier-Stokes method with the goal to meet engine manufacturer requirements by design optimization. Performance prediction and flowfield analysis of a rotor in hover by application of a coupled Euler/Boundary Layer method was presented by Beaumier et al. [3].

In 1997, a development program was started at EUROCOPTER DEUTSCHLAND (ECD) to upgrade the BK117-C1 helicopter currently in service to the new BK117-C2 helicopter with first deliveries in 2000. This upgrade includes the redesign of the fuselage in order to increase the cabin volume. Due to the restricted program time scale and the high costs of an extensive wind tunnel test campaign it was decided to perform only simple wind tunnel tests for evaluating the aerodynamic coefficients of the redesigned BK117-C2 fuselage and to supplement these tests by CFD calculations using a commercial CFD software. This paper deals with the first CFD applications at ECD during the fuselage design phase of the upgrade helicopter BK117-C2.

The BK117 upgrade development program has entered the flight testing phase with the first prototype taken off to its maiden flight in June 1999. Furthermore, it was decided to give the BK117-C2 upgrade helicopter its official name EC145, which is now used for the remainder of the paper.

## Aerodynamic Design of the EC145

Based on the BK117 helicopter, which was developed from 1978 to 1982 in a cooperation between ECD (formerly Messerschmitt-Bölkow-Blohm (MBB)) and Kawasaki Heavy Industries (KHI), this cooperation was renewed to develop the EC145. The main technical features of the EC145 are

- a new fuselage shape with increased length and width for increased payload volume and improved accessibility,
- a completely new cockpit design based on the EC135 helicopter including advanced avionics,
- rotor blades with advanced planform and modern airfoils for increased performance, and
- new hydraulics and a new control system using flexballs for connecting pilot controls and hydraulic actuators.

The complete upper deck including engine, gearbox and dynamic system as well as tail boom, vertical fin and tail rotor were left unchanged.

The aerodynamic and aeroacoustic layout of the new rotor blades and first results of flight tests on a BK117 test helicopter were presented by Bebesel et al. [4]. Besides the improved performance, a low noise radiation could be confirmed for the new EC145 rotor blades.

The design of the EC145 fuselage shape required the investigation of the aerodynamic characteristics to provide information on fuselage airloads and flight stability for the upgrade helicopter. For the determination of the fuselage aerodynamic coefficients in the full incidence and sideslip angle range measurements using a 1:5 scaled model were performed in the EUROCOPTER wind tunnel at Marignane in July 1997 (Reymond et al. [5]). The increased cabin volume and the new cockpit shape changed the fuselage contribution to the aerodynamic stability of the EC145. To retain the same stability characteristics as for the BK117, the horizontal stabilizer and the endplates had to be adapted. Therefore, the CFD flow simulations of the EC145 fuselage should supplement the wind tunnel tests in order to provide

- an accurate prediction of the surface pressure distributions for the determination of airloads for stress analysis of local fuselage parts such as doors and windows, and
- an estimation of the horizontal stabilizer pitching and endplates yawing efficiencies for design changes of the empenage.

## Choice of Numerical Method

The choice of the numerical method used for the CFD simulation of the EC145 fuselage was based on industrial and technical requirements:

- The CFD software should have an user-friendly graphical interface and a good documentation to reduce user training and speed-up the handling.
- Maintenance of the CFD software and user support should be guaranteed.
- The CFD software has to be parallized and capable of running efficiently on workstation clusters since this is the only hardware configuration affordable and available at EUROCOPTER.
- A flexible post-processing should allow for an extensive flowfield analysis and load integration.
- The complex fuselage and empenage geometry ask for a flexible and efficient grid generation strategy. This can only be fulfilled by using the unstructured grid approach.

- The freestream velocities encountered by the fuselage are below Ma = 0.3 and therefore the incompressible flow model is best suited for fuselage flow simulations.
- The CFD method should converge fast and accurately predict the surface pressure distribution.

During an European research project it was demonstrated that commercially available unstructured CFD methods are mature to fulfill the requirements listed above and that accurate predictions of fuselage surface pressure distributions can be obtained (Costes et al. [6]). After an assessment of some commercial CFD methods, the FLUENT/UNS software [7] was chosen and introduced in the aerodynamic department of ECD. FLUENT/UNS solves the incompressible Navier-Stokes equations for conservation of mass and momentum on unstructured grids with additional conservation equations for the turbulent kinetic energy and dissipation in order to model turbulent flows. Furthermore, the FLUENT/UNS software offers the possibility to introduce an actuator disk model into the computational domain which allows for consideration of the influence of main rotor downwash on the fuselage and empenage aerodynamics.

Since the simulations reported in this paper were the first of this type performed at ECD, no attempt has been made to adapt or optimize turbulence modeling. For all calculation reported herein the standard k-ε model with default parameters has been selected. Furthermore, the hardware resources available at ECD restricted the number of grid points. Hence, the obtained grid resolution was inadequate for accurately predicting viscous and turbulent effects and an accurate simulation of flow separation, skin friction, and drag forces was therefore not expected.

## CFD Method Validation by BK117 Fuselage Flow Simulations

Before stepping into the aerodynamic simulation of the EC145 fuselage, the chosen CFD method FLUENT/UNS was validated by calculating the flowfield around the present BK117 fuselage. For this fuselage, wind tunnel measurements including surface pressure data are available, which were acquired during wind tunnel test campaigns in 1978 and 1981 by KHI (Nakano et al. [8], [9]). To support the introduction of FLUENT/UNS into ECD, the company FLUENT DEUTSCHLAND performed demonstrative flow calculations for the BK117 fuselage. The geometrical surface description of the BK117 fuselage was given to FLUENT DEUTSCHLAND as a CAD surface description. A geometry model suitable for CFD flow simulations was created by removing gaps and overlaps of the CAD surface and by closing the engine inlets and exhaust outlets. The final BK117 fuselage geometry is shown in Figure 1 together with the computational domain as defined by FLUENT DEUTSCHLAND.

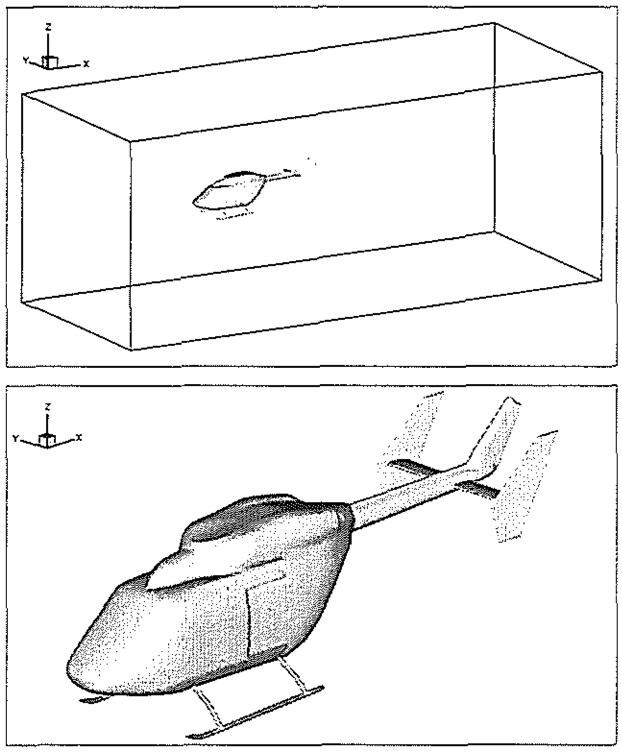

Figure 1: Computational domain and geometrical model for the BK117 fuselage flow simulation.

For generation of the surface grid depicted in Figure 2, the ANSA software was used which allows for a fast and efficient triangulation of the complex fuselage surface with a high degree of automatisation. The tetrahedrals of the volume grid were generated using TGRID, which is part of the FLUENT/UNS software package. The final grid consists of 86.000 surface triangles and 500.000 tetrahedral volume elements.

For method validation, three different flow conditions were selected. Zero incidence and zero sideslip angle $\alpha = 0°$, $\beta = 0°$ was considered as reference case. One high incidence angle case ($\alpha = -15°$, $\beta = 0°$) and one high sideslip angle case ($\alpha = 0°$, $\beta = 10°$) should verify the CFD method accuracy at the limits of operational flight range. Flow computations were converged up to a residual drop of 3 to 4 orders of magnitude and the convergence of the pressure field was assured by monitoring the change in overall fuselage lift coefficient.

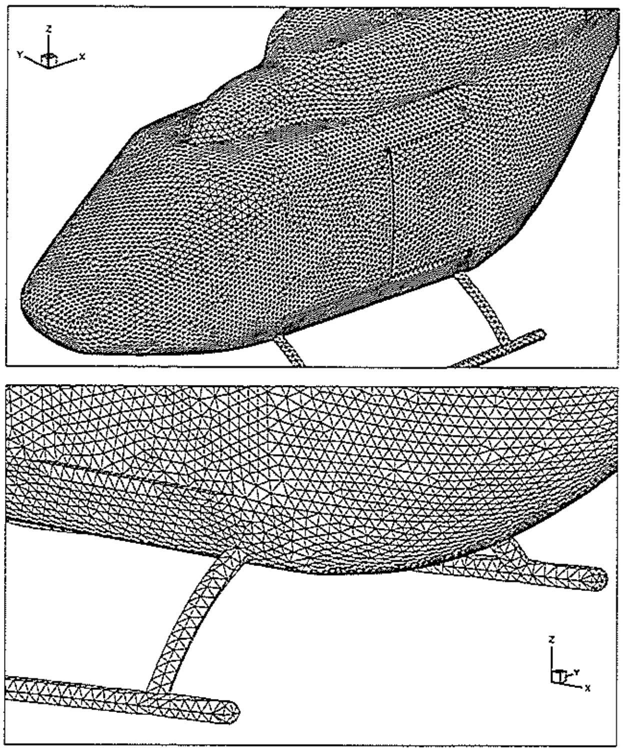

Figure 2: Details of the BK117 fuselage surface grid.

Figure 3 depicts a sketch of the cross sections for which the comparisons of calculated and measured surface pressure distributions are presented.

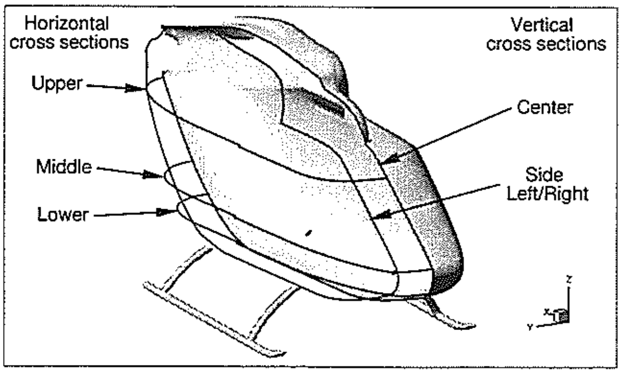


Figure 3: Analyzed cross sections for pressure coefficient distributions.

Reference Case: $\alpha = 0°$, $\beta = 0°$

The flow condition with zero incidence and zero sideslip angle was chosen as reference case for setting up, investigating and verifying the parameters defining convergence behavior and accuracy of FLUENT/UNS.

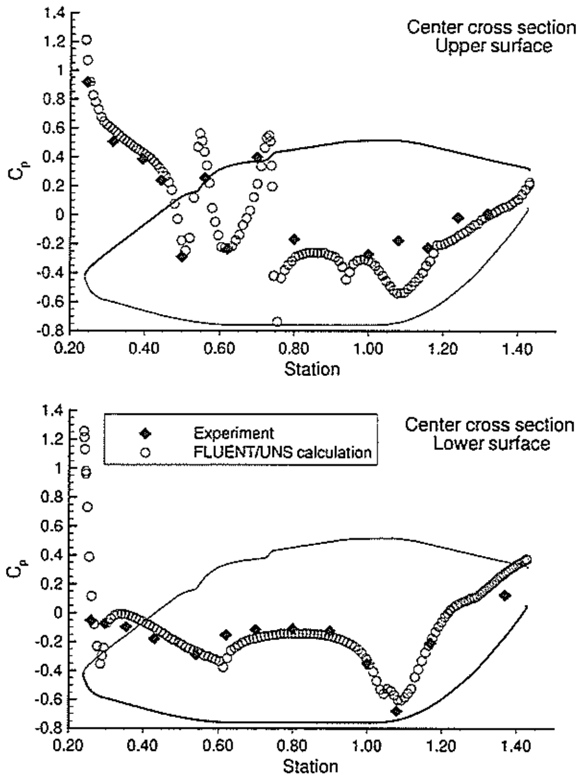


Figure 4: Pressure coefficient distributions at center cross section ($\alpha=0°$, $\beta=0°$).

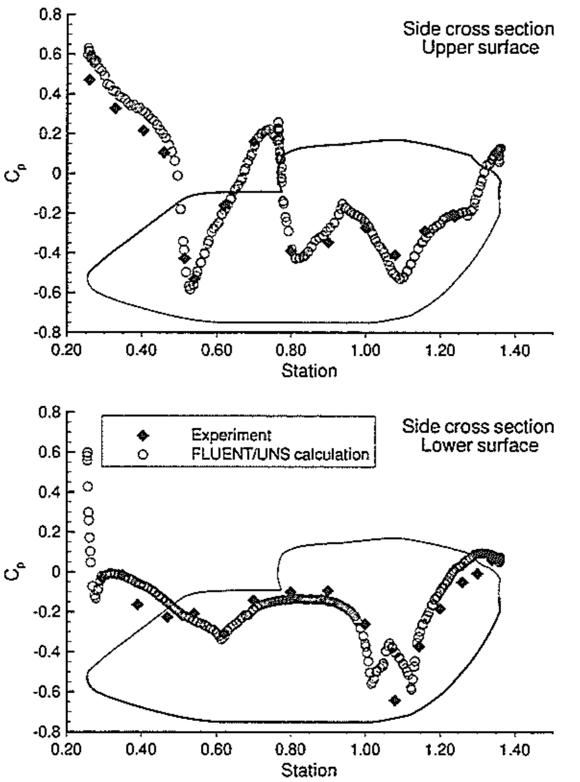


Figure 5: Pressure coefficient distributions at side cross section ($\alpha=0°$, $\beta=0°$).

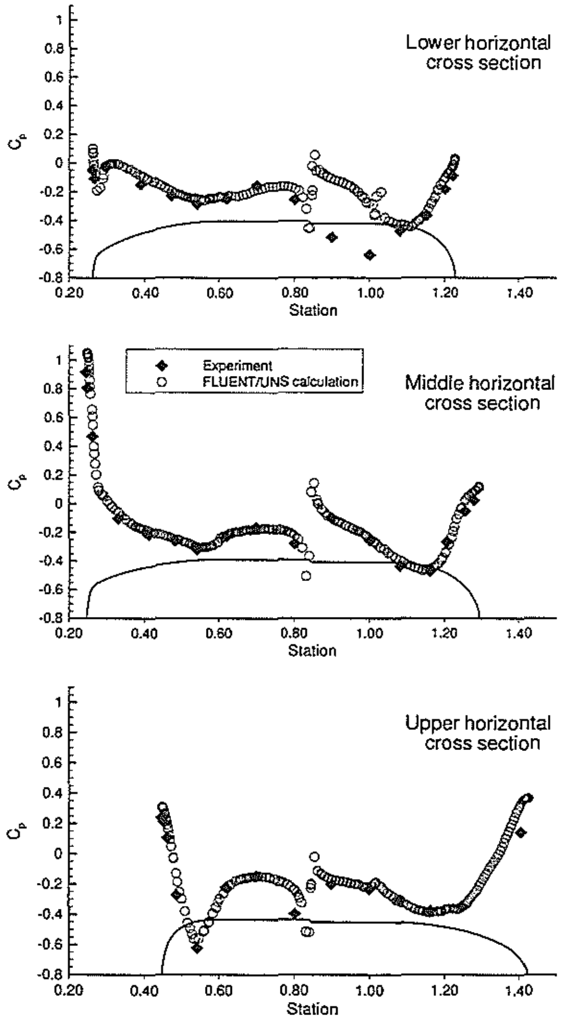


Figure 6: Pressure coefficient distributions at horizontal cross sections ($\alpha$=0°, $\beta$=0°).

The comparison of calculated and measured pressure coefficient distributions in vertical and horizontal cross sections are presented in Figures 4, 5, and 6, respectively. The overall agreement between CFD simulation results and experimental data is very good.

A more detailed analysis reveals that the discrepancies found in the aftbody region on the lower surface (Figures 4, 5) are due to low grid resolution combined with an insufficient turbulence modeling. The pressure level on the aftbody (clamshell doors) is predicted too high and the suction peak in the high curvature region at the beginning of the aftbody is not correctly resolved.

In contrast to the CFD model, the wind tunnel model was equipped with a rotating rotor hub including blade stubs. Therefore, the calculated pressure distribution on the upper surface deviates from the measured values after station 1.0 (upper part of Figure 4).

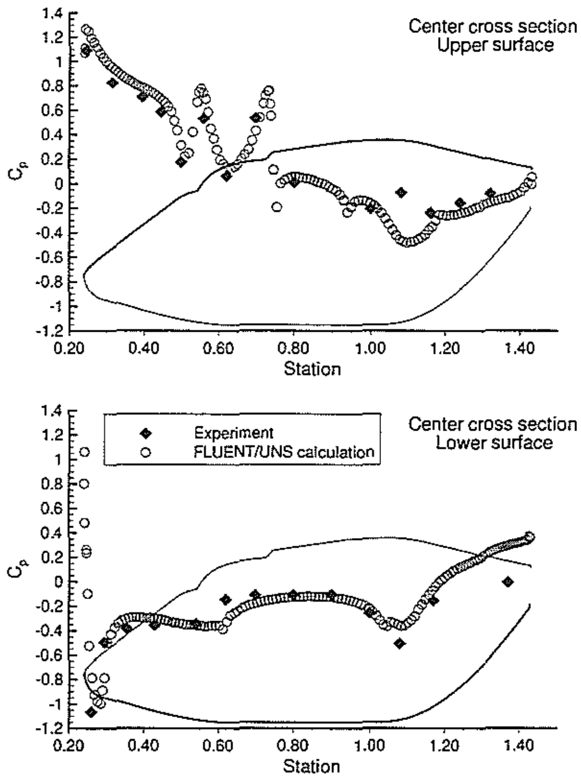


Figure 7: Pressure coefficient distributions at center cross section ($\alpha$=-15°, $\beta$=0°).

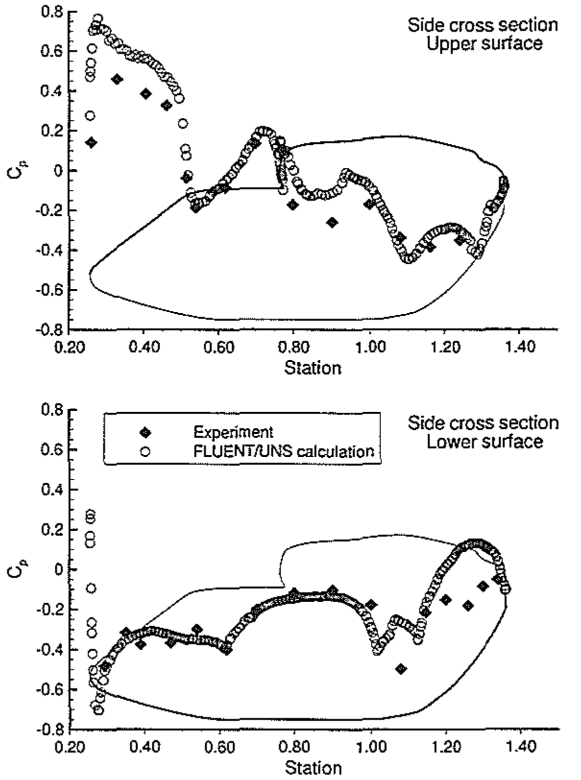


Figure 8: Pressure coefficient distributions at side cross section ($\alpha$=-15°, $\beta$=0°).

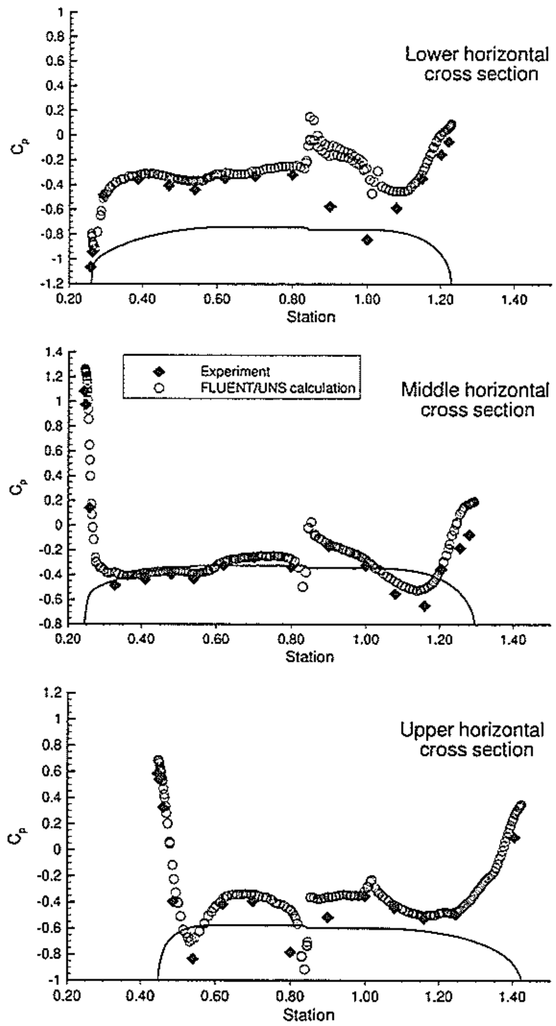


Figure 9: Pressure coefficient distributions at horizontal cross sections ($\alpha$=-15°,$\beta$=0°).

The discrepancies found in the nose region for the side vertical cross section can be explained by inadequate grid resolution of the high geometrical curvature in horizontal direction. Due to the layout of the Figures, these differences can not be clearly identified in the pressure distributions of the horizontal cross sections (Figure 6).

Finally, the big differences at the lower horizontal cross section between stations 0.8 and 1.0 are attributed to a different geometrical representation of the sliding door attachment in the computational model and the wind tunnel model.

## High Incidence Angle Case: $\alpha$ = -15°, $\beta$ = 0°

Fuselage flow conditions with high incidence angles are usually encountered during climb or due to main rotor downwash in very low speed flight.

The calculated and measured pressure distributions for the vertical cross sections are shown in Figures 7 and 8, and for the three horizontal cross sections in Figure 9.

For the comparison of CFD simulation results and experimental data, the same conclusions as for the reference case can be drawn: a good overall agreement but increased differences in high curvature regions due to insufficient grid resolution and turbulence modeling. The high freestream incidence pronounces the discrepancies in the nose region at the side vertical cross sections and on the fuselage aftbody.

## High Sideslip Angle Case: $\alpha$ = 0°, $\beta$ = -10°

In contrast to fixed-wing fuselages, helicopter fuselages often operate under high sideslip angles occurring during sideward flight or low speed trimming with zero bank angle.

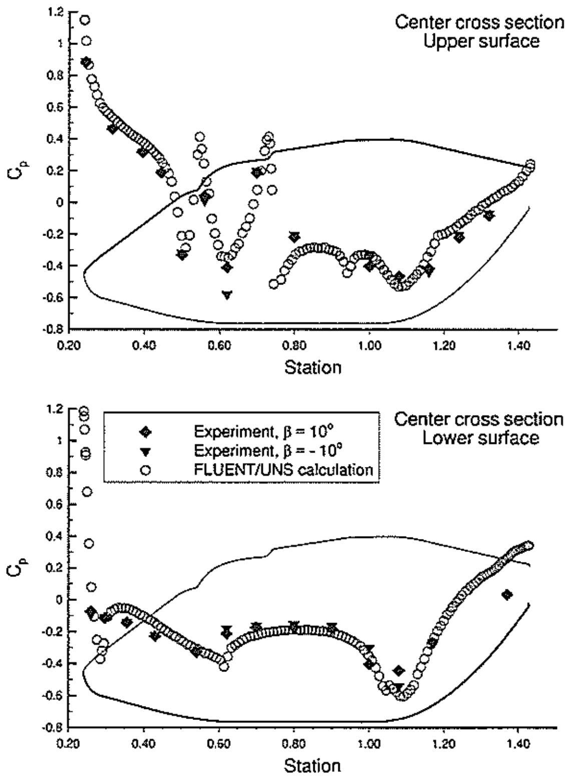


Figure 10: Pressure coefficient distributions at center cross section ($\alpha$=0°, $\beta$=-10°).

Figures 10, 11, 12 and 13 show the pressure distributions for the cross sections defined in Figure 3. Since the fuselage shape is symmetrical up to the tail boom, the calculated pressure results in the center cross section are compared to experimental values for the wind tunnel cases with positive ($\alpha$ = 0°, $\beta$ = 10°) and negative ($\alpha$ = 0°, $\beta$ = -10°) sideslip angle. Furthermore, results for both right and left side cross sections are presented.

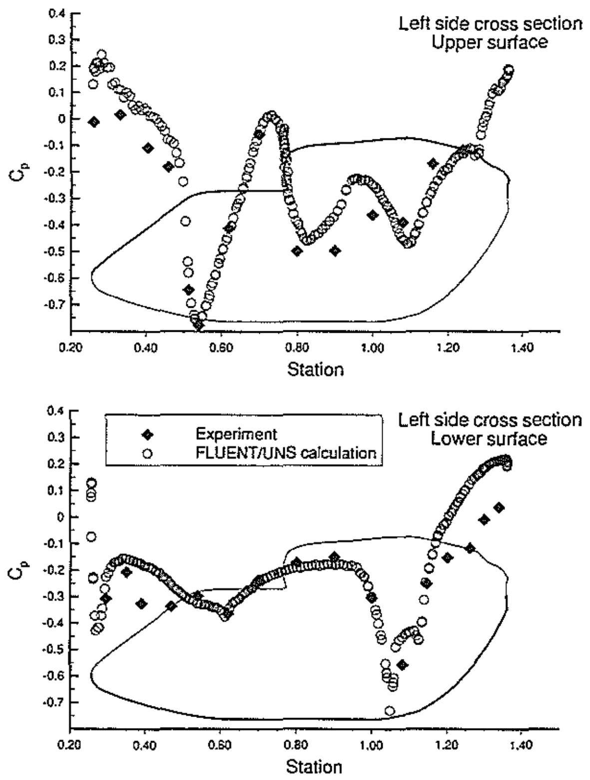


Figure 11: Pressure coefficient distributions at left side cross section ($\alpha$=0°, $\beta$=-10°).

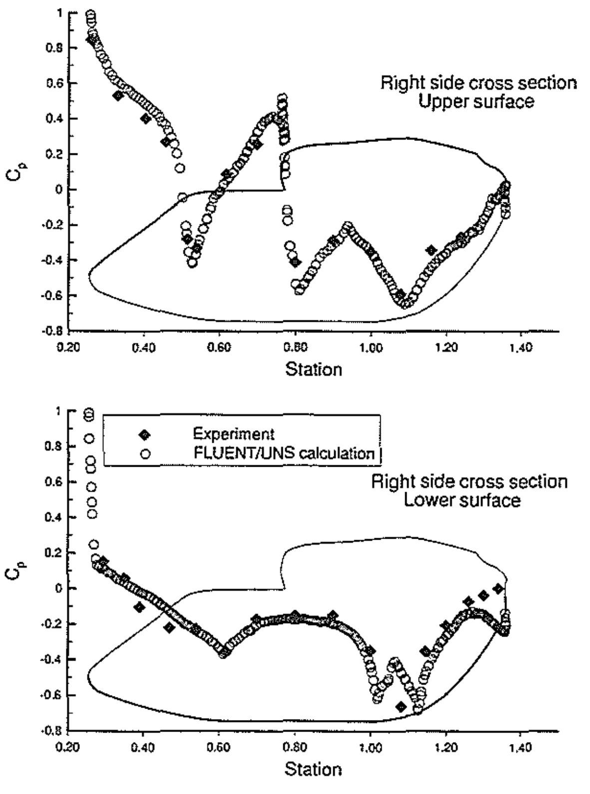


Figure 12: Pressure coefficient distributions at right cross section for $\alpha$=0° and $\beta$=-10°.

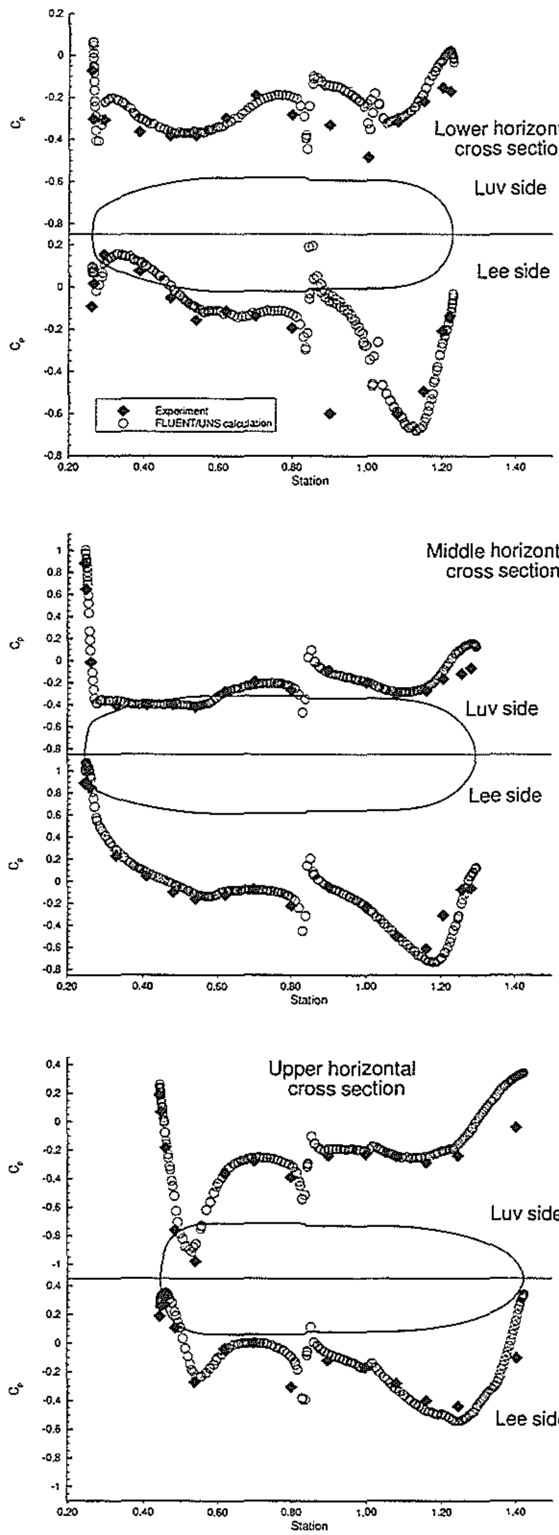


Figure 13: Pressure coefficient distributions at horizontal cross sections ($\alpha$=0°,$\beta$=-10°).

As for the previous two validation test conditions, the overall agreement between measurements and calculation results is good. Problem areas with greater discrepancies are again high curvature regions at the cockpit and the aftbody. The comparison of pressure distributions for the horizontal cross sections prove, that the CFD method is able to accurately simulate the flowfield on the luv side as well as on the lee side of the fuselage.

Prediction of Horizontal Stabilizer Efficiency

The CFD method validation was concluded with an assessment of the ability to predict the lift efficiency of the BK117 horizontal stabilizer and its contribution to the BK117 fuselage pitching moment. The pitching moment contribution of the horizontal stabilizer does not only influence the aircraft's stability and handling qualities, but also determines the pitching moment to be produced by the main rotor and thus the rotor shaft loading.

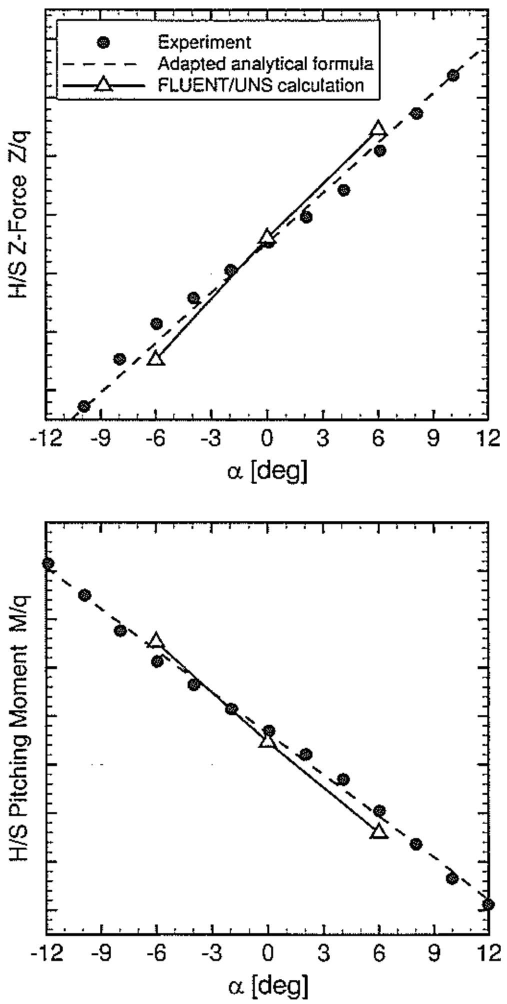


Figure 14: BK117 horizontal stabilizer Z-force and pitching moment contribution.

In Figure 14 the BK117 horizontal stabilizer (H/S) force in fuselage z-direction and the H/S pitching moment contribution predicted by the CFD calculations are compared to the results of the wind tunnel tests (Nakano et al. [8]). As ordinate the fuselage freestream incidence angle is used. The H/S force and pitching moment contribution were obtained by integrating the calculated pressure distribution on the horizontal stabilizer using the corresponding tool of the FLUENT/UNS software.

In contrast to the CFD model, the wind tunnel model was equipped with a fixed rotor hub and small blade stubs. Despite the missing hub wake influence in the CFD simulations, the agreement between calculated values and wind tunnel data is very good. The H/S pitch efficiency, which is determined by the slope of the pitching moment curve, is predicted to be slightly higher than obtained by experiment. Obviously, the CFD method is able to account correctly for the influence of the fuselage wake on the H/S aerodynamics.

For the pre-design of the EC145 horizontal stabilizer, simple analytical formulas for estimating the H/S lift curve slope and pitch stability contribution were used (Hoerner and Borst [10]). All wake and interference effects were taken into account by introducing efficiency factors which were adapted to the BK117 wind tunnel test data. The results obtained by these adapted analytical formulas are also shown in Figure 14.

**EC145 Fuselage Flow Simulations**

The geometrical definition of the EC145 fuselage shape was prepared as a CATIA model by the ECD pre-design department. In the aerodynamics department, this model was revised to remove all CAD surface gaps and overlaps and supplemented by closure surfaces for engine inlets and exhaust outlets. Furthermore, the main rotor disk plane was introduced in order to allow for activation of the FLUENT/UNS actuator disk model. The computational domain was increased compared to the BK117 simulation model to reduce as much as possible any farfield influence on the calculation results. Figure 15 presents the computational domain and the final geometry of the EC145 fuselage CFD model.

The surface grid generation was performed using PCUBE, a grid generation software developed by ICEM CFD which is included in the FLUENT/UNS software package. Although the graphical user interface of PCUBE greatly facilitates the set-up of the surface grid generation process, the computational time required and the low quality of the triangularisation at high curvature regions deteriorates much the efficiency of the unstructured grid generation.

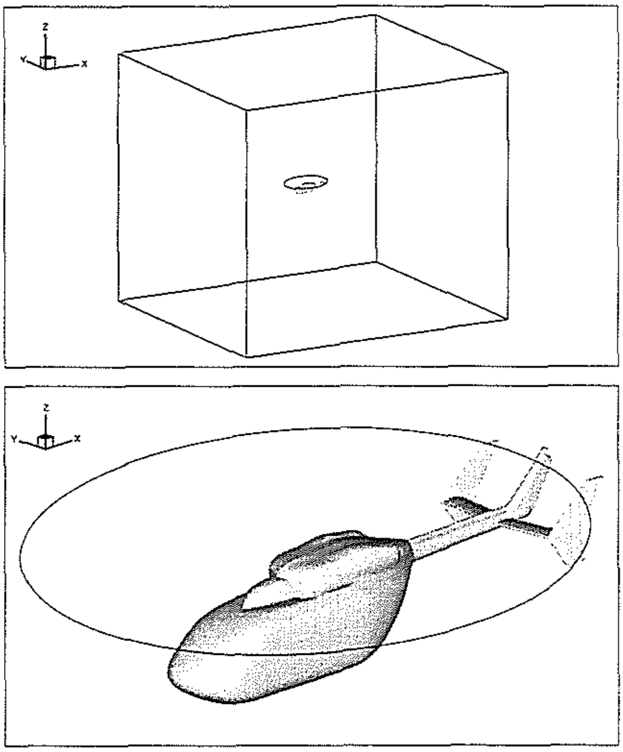

Figure 15: Computational domain and geometry model with main rotor actuator disk for EC145.

Since the goal of the EC145 fuselage flow simulations was not only to provide pressure distributions on the fuselage surface, but to assess the capability of estimating empenage aerodynamic loads by CFD methods, the surface grid was refined on the horizontal stabilizer (H/S) and the endplates (E/P) as shown in Figure 16.

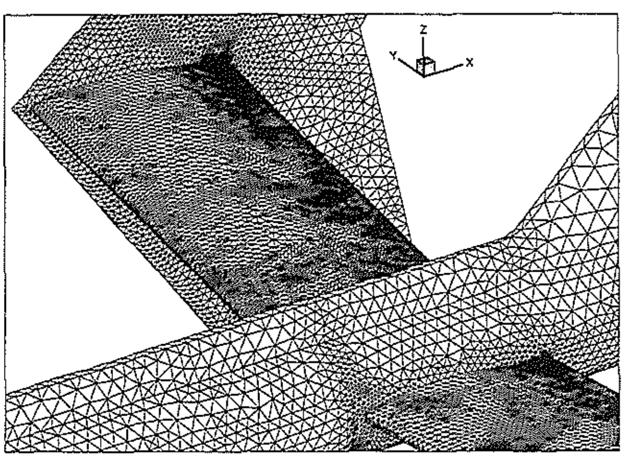

Figure 16: EC145 fuselage surface grid detail.

The finally obtained surface grid consists of 51.000 triangles and the volume grid produced automatically without any user input by TGRID contains 363.000 tetrahedral elements.

Flow calculations using the same parameter set-up as for the BK117 validation cases were run for various flight conditions covering the full incidence and sideslip angle range of a helicopter. All computations were converged up to a residual drop of about 3 orders of magnitude and the monitoring of the overall lift coefficient was used as an indicator of the level of pressure field convergence.

## Prediction of Surface Pressure Distributions

For demonstration purposes, Figures 17 and 18 show calculated pressure distributions at the center vertical cross section and two horizontal cross sections for an incidence angle of $\alpha$ = -18° and a sideslip angle of $\beta$ = 10°. This is a representative flight condition for a push-over maneuver which is one of the extreme cases for limit load estimation and stress analysis of the fuselage structure. The predicted pressure distributions are supposed to have the same inaccuracies in the high curvature regions cockpit and aftbody as found in the BK117 validation.

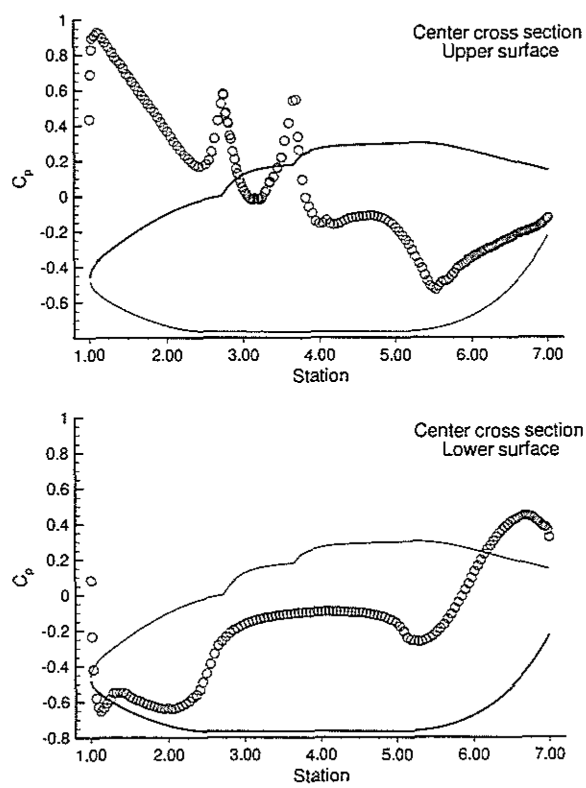


Figure 17: Pressure coefficient distributions at center cross section ($\alpha$=-18°, $\beta$=10°).

All calculated surface pressure distributions were provided to the stress analysis department and used as air pressure load input for

- FEM simulations and stress analysis of the fuselage structure,
- FEM simulations and determination of the necessary thickness of the wind screen Plexiglas window, and
- stress analysis and structural design of side windows, sliding and clam shell doors.

Furthermore, a preliminary definition of the location of the static ports for altimeter and flight speed indicator could be made based on the calculated pressure distributions.

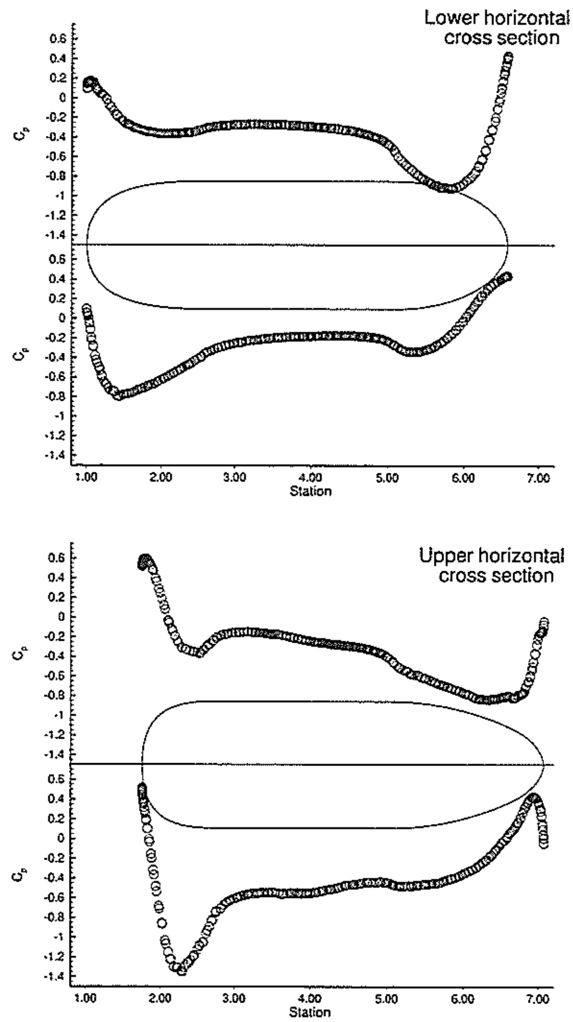


Figure 18: Pressure coefficient distributions at horizontal cross sections (α=-18°, β=10°).

## Prediction of Empenage Efficiencies

Compared to the BK117, the new fuselage shape changes the aerodynamic stability of the EC145 helicopter. In order to retain or even improve the BK117 stability characteristics, the EC145 horizontal stabilizer (H/S) and endplates (E/P) have to be redesigned.

Using the simple analytical formulas adapted to the BK117 wind tunnel results, a first version of the EC145 empenage was defined and tested in the wind tunnel (see Reymond et al. [5]). Figure 19 shows the analytically predicted slopes of H/S lift force and pitching moment efficiency in very good agreement with the measured aerodynamic coefficients. In this and the following Figures, α and β denote the fuselage freestream incidence and sideslip angles.

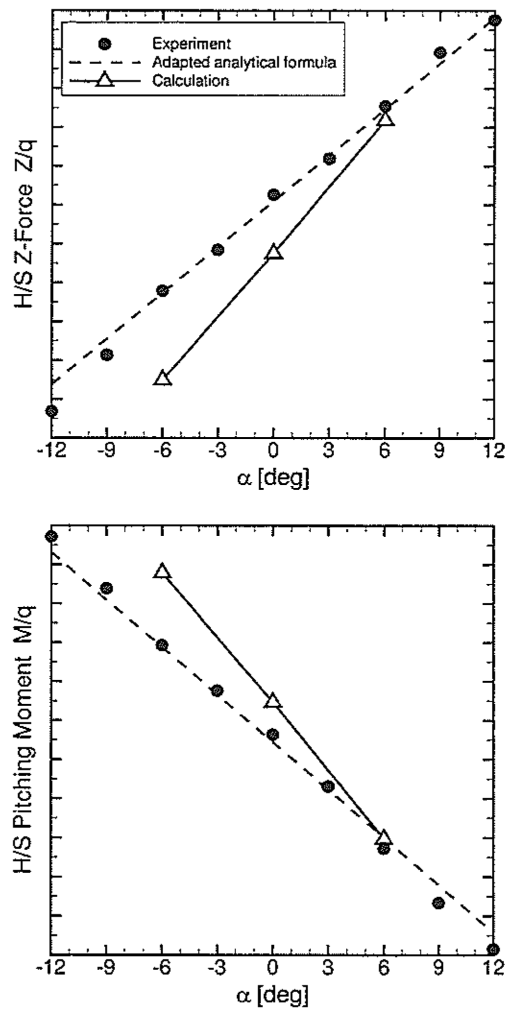


Figure 19: EC145 horizontal stabilizer Z-force and pitching moment contribution, old design.

For three incidence angles the H/S force and moment values were extracted from the CFD simulation results. The calculated coefficients for α = 6° are very close to the experimental data, but for α = 0° and α = -6° the gap between CFD calculation and wind tunnel data increases. In the wind tunnel experiment, the model was equipped with a rotating hub and comparatively large blade stubs. Therefore, the difference between calculation and experiment may be explained by the missing rotor hub wake in the CFD computations, since for negative incidence angles this wake starts to interact with or even impinges on the H/S. If the EC145 results are compared to BK117 validation (Figure 14), the hub rotation and the increased size of the blade stubs seem to significantly influence the estimation of the H/S aerodynamics.

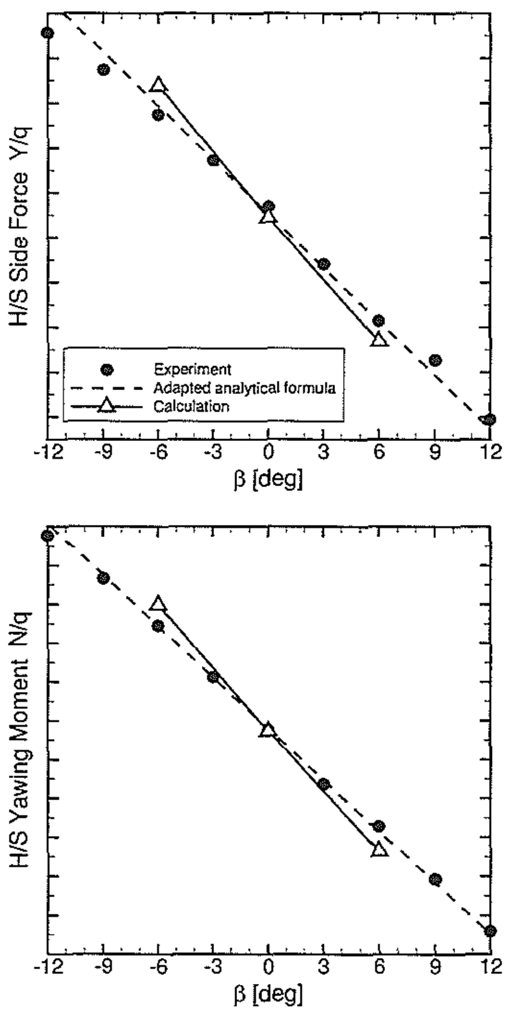


Figure 20: EC145 endplates side force and yawing moment contribution, old design.

Figure 20 presents the slopes of E/P side force and yawing moment as predicted by the adapted analytical formulas together with the aerodynamic coefficients measured in the wind tunnel and calculated by the CFD simulations. With the analytical formulas the slopes measured later-on in the wind tunnel tests were accurately predicted.

The agreement of the CFD results and the experimental data is very good and much better than for the H/S. This supports the explanation of the missing rotating hub wake causing the differences in calculated and measured H/S aerodynamic coefficients, since these wake effects are not experienced by the E/P. For zero sideslip angle ($\beta$ = 0°), the experimental E/P force and moment coefficients were accurately simulated while the slopes are slightly overpredicted by the CFD method.

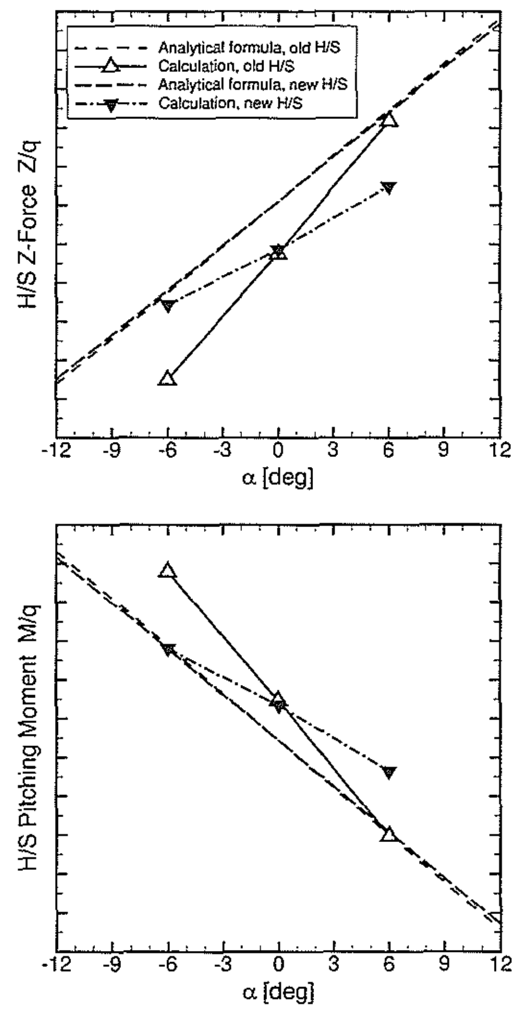


Figure 21: EC145 horizontal stabilizer Z-force and pitching moment contribution, new design.

Unfortunately, some design changes of the H/S and E/P were necessary due to structural and design constraints during the development phase of the EC145. By using the adapted analytical formulas, the geometry of the new empenage was designed to have equal aerodynamic efficiencies as the old one. The new H/S was increased in span and has a smaller chord. For the new E/P, the leading edge back sweep of the upper and lower part was increased. The final H/S and E/P designs were introduced in the CFD geometry model, the computational grid was regenerated and flow calculations were performed in order to analyze more accurately the differences in aerodynamic efficiencies caused by the redesign.

Calculated lift force and pitching moment coefficients for the new H/S design are compared to the results for the old version in Figure 21. The aerodynamic efficiency, characterized by the force and moment slopes, is reduced significantly by the new H/S design. Currently, no explanation can be found for this unexpected behavior and a more detailed analysis will be performed to investigate the cause of this H/S efficiency deterioration.

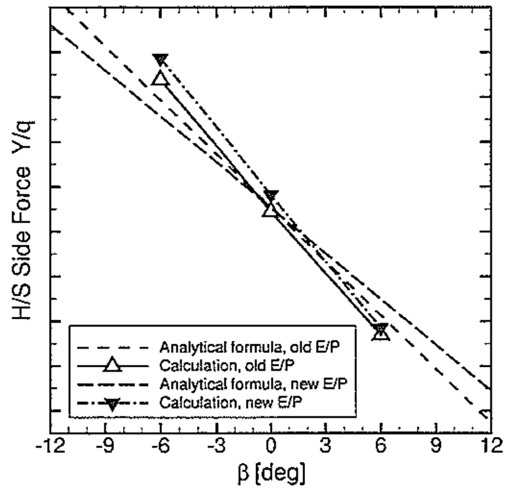


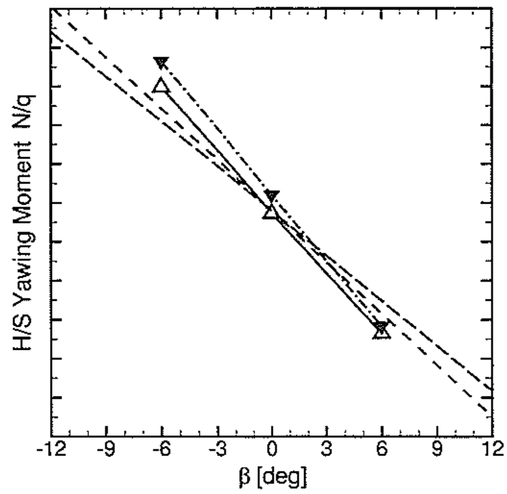


Figure 22: EC145 endplates side force and yawing moment contribution, new design.

Figure 22 shows the CFD prediction results for the aerodynamic characteristics of the old and new E/P versions. It is clearly demonstrated that the objective not to change the E/P efficiency by the redesign was reached, although the trend of efficiency reduction by the new design as indicated by the analytical formulas is reversed in the CFD results. Nevertheless, the differences in aerodynamic coefficients of both E/P designs are small and should not change the analysis concerning helicopter loads and handling qualities for the yaw axis.

Simulation of Main Rotor Downwash Influence

Finally, CFD simulations were performed to investigate the influence of main rotor downwash on the aerodynamic coefficients of the horizontal stabilizer. FLUENT/UNS provides an actuator disk model with the possibility to specify arbitrary pressure jump distributions across a predefined surface. In a first attempt to activate this model, a constant pressure jump distribution derived from the main rotor thrust was prescribed in the main rotor disk plane (see Figure 15). Although this approach does not account for the strong tip downwash velocities induced by the tip vortices of the main rotor blades, the averaged influence of the main rotor induced velocity field on the integrated aerodynamic H/S loads should be captured.

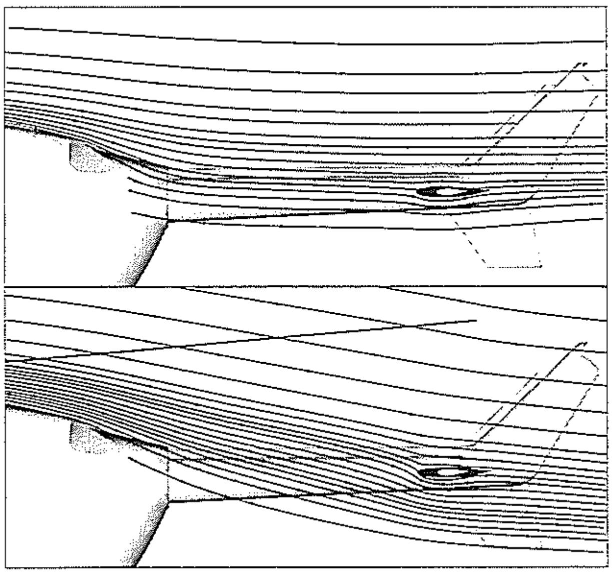

Figure 23: Streamlines in a vertical cross section plane for a CFD simulation of the EC145 fuselage with and without main rotor actuator disk model.

The effect of the main rotor actuator disk model is visualized by the streamlines drawn in Figure 23 for the flow case $\alpha = 0°$ and $\beta = 0°$. Due to the rotor-induced downwash velocity field the local H/S incidence angle is strongly changed.

The effect on the aerodynamic efficiency of the H/S is presented in Figure 24. As expected, the change in local H/S incidence angle causes the H/S to produce much more downlift and thus a higher pitching moment contribution. Furthermore, the linear correlation between H/S force or moment coefficient and fuselage freestream incidence angle is no longer valid and non-linear effects are introduced by the rotor downwash.

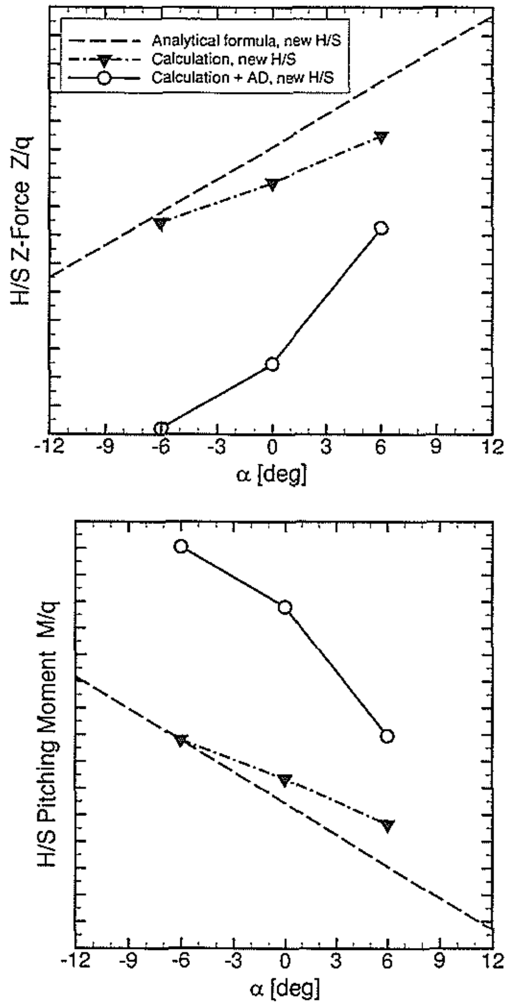


Figure 24: EC145 horizontal stabilizer Z-force and pitching moment contribution, influence of rotor downwash.

These results clearly demonstrate the importance of incorporating a model for the main rotor downwash velocity field into fuselage CFD simulations to be able to reliably predict horizontal stabilizer efficiencies for helicopters.

## Conclusions

At EUROCOPTER DEUTSCHLAND the commercial CFD software FLUENT/UNS was introduced into the industrial design process and was used for the first time in the EC145 development program. The CFD method was extensively validated by simulating the BK117 fuselage flowfield. The accuracy of the predicted surface pressure was found to be good and the calculated empenage aerodynamic load coefficients show a satisfactory agreement with wind tunnel data. EC145 fuselage CFD simulations supplemented the wind tunnel test by providing surface pressure distributions, by estimating horizontal stabilizer and endplates efficiencies and by investigating the aerodynamic influence of empenage redesign and main rotor downwash.

The main conclusions regarding the technical results obtained using the commercial CFD method FLUENT/UNS are:

- a good and robust convergence of the numerical scheme.
- surface pressure distributions can be reliably predicted in the full incidence and sideslip angle range and were successfully utilized as input for stress analysis of fuselage structure.
- aerodynamic efficiencies of endplates can be calculated with sufficient engineering accuracy for design purposes.
- the prediction of horizontal stabilizer aerodynamic efficiencies depend strongly on the incorporation of all interaction effects such as those induced by rotating rotor hub wake and main rotor downwash.

Further work at ECD on fuselage CFD simulation will be devoted to

- a more detailed analysis and improved prediction of the interactional aerodynamics of horizontal stabilizers,
- a more refined main rotor actuator disk modeling employing realistic pressure jump distributions in the rotor disk plane, and
- incorporation of the tail rotor as actuator disk model in order to investigate the influence of tail rotor induced velocities on endplates.

For the prediction of fuselage drag and other flow features associated with viscous effects the pure unstructured approach seems to be not suitable due to the enormous number of grid elements required to resolve boundary layers. The current developments dealing with the hybrid approach employing prisms in the boundary layer looks promising and attempts will be made in the future towards first applications to helicopter fuselages.

Regarding the efficiency enhancement of the industrial design process by the introduction and application of a CFD method it can be concluded that

- the geometry modeling for CFD applications should be improved by taking into account the requirements of CFD in the construction of the CAD models,
- the unstructured approach strongly facilitate the grid generation task for the complex geometry of a helicopter fuselage,
- the performance of the PCUBE tool and the time required for surface grid generation is not acceptable and has to be improved (in fact it was reported that the current unstructured grid generator tool of ICEM CFD has an appreciable enhanced performance compared to PCUBE),
- the graphical user interface of FLUENT/UNS allows for an easy selection of all parameters and fast set-up of calculations even for an inexperienced user,
- for some analysis the post-processing tool of FLUENT/UNS turns out to be insufficient, but a lot of interfaces to common and powerful visualization and analysis tools (e.g. TECPLOT) overcome this drawback.

Although there are things to improve, the CFD capability enabled ECD to strongly accelerate the aerodynamic design process of the EC145 fuselage and a significant amount of time and cost for wind tunnel tests was saved.

In order to further enhance its aerodynamic prediction capabilities, EUROCOPTER in cooperation with the French and German research establishments ONERA and DLR started a long-term research project called CHANCE in July 1998. The main goal of this research partnership is the development, validation and industrialization of a CFD method capable to simulate the flow fields around isolated helicopter components (main rotor, fuselage, tail rotor) as well as around the complete helicopter.

**Acknowledgements**

The author would like to thank Dr. H. Rexroth and W. Seibert from FLUENT DEUTSCHLAND for preparing the BK117 fuselage geometry model, for generating the BK117 computational grid, and for performing demonstrative test calculations. Furthermore, W. Seibert's assistance during the first EC145 calculations is acknowledged.

## REFERENCES

[1] HASSAN A.A., THOMPSON T., DUQUE E.P., MELTON J.
Resolution of Tail Buffet Phenomena for AH-64D Longbow Apache: A Case Study on the Application of a Modern CFD Analysis Tool for Improved Helicopter Aerodynamic Design
*Proceedings of the 52nd Annual Forum of the American Helicopter Society, 1997.*

[2] SERR CH., CANTILLON M.
Navier-Stokes Calculation: An Industrial Tool for Air Intake Optimization
*Paper No. 93, Proceedings of the 22nd European Rotorcraft Forum, Brighton, UK, 1996.*

[3] BEAUMIER P., CASTELLIN C., ARNAUD G.
Performance Prediction and Flowfield Analysis of Rotors in Hover Using a Coupled Euler/Boundary Layer Method
*Paper No. AE12, Proceedings of the 24th European Rotorcraft Forum, Marseilles, France, 1998.*

[4] BEBESEL M., POLZ G., SCHÖLL E.
Aerodynamic and Aeroacoustic Layout of the ATR (Advanced Technology Rotor)
*Proceedings of the 55th Annual Forum of the American Helicopter Society, Montreal, Canada, 1999.*

[5] REYMOND J., TONOLLI B., MISTRAL L.
BK117-C1/-C2 Wind Tunnel Tests
*Internal Report E/IM.E No. 3388, Eurocopter, September 1997*

[6] COSTES M., COLLERCANDY R., KROLL N., FRHR. VON GEYR H., RENZONI P., AMATO M., KOKKALIS A., ROCCHETTO A., SERR C., LARREY E., FILIPPONE A., WEHR D.
Navier-Stokes Calculations of Helicopter Fuselage Flowfield and Loads
*Proceedings of the 54th Annual Forum of the American Helicopter Society, Washington, D.C., 1998.*

[7] User's Guide for FLUENT/UNS and RAMPANT
*Release 4.0, Vol. 1-3, Fluent Incorporated, April 1996.*

[8] NAKANO M., IKEBE Y.
Wind Tunnel Test Result of BK117 Airframe – Test Series 3 –
*Internal Report KKA-78-088, Kawasaki Heavy Industries, 1978.*

[9] NAKANO M., IKEBE Y., MIYAJIMA K.
Pressure Distributions of BK117 Airframe – Wind Tunnel Test Report –
*Internal Report KKA-81-211, Kawasaki Heavy Industries, 1981.*

[10] HOERNER S.F., BORST H.V.
Fluid-Dynamic Lift
*published by L.A. Hoerner, Hoerner Fluid Dynamics, Brick Town, N.J., 1975*